# Spectral Subtraction of Robot Motion Noise for Improved Event Detection in Tactile Acceleration Signals

William McMahan and Katherine J. Kuchenbecker

Haptics Group, GRASP Laboratory
Department of Mechanical Engineering and Applied Mechanics
University of Pennsylvania, Philadelphia, USA
{wmcmahan,kuchenbe}@seas.upenn.edu
http://haptics.seas.upenn.edu

**Abstract.** New robots for teleoperation and autonomous manipulation are increasingly being equipped with high-bandwidth accelerometers for measuring the transient vibrational cues that occur during contact with objects. Unfortunately, the robot's own internal mechanisms often generate significant high-frequency accelerations, which we term ego-vibrations. This paper presents an approach to characterizing and removing these signals from acceleration measurements. We adapt the audio processing technique of spectral subtraction over short time windows to remove the noise that is estimated to occur at the robot's present joint velocities. Implementation for the wrist roll and gripper joints on a Willow Garage PR2 robot demonstrates that spectral subtraction significantly increases signal-to-noise ratio, which should improve vibrotactile event detection in both teleoperation and autonomous robotics.

**Key words:** haptic feedback for teleoperation, vibrations, tactile accelerations, noise suppression

## 1 Introduction

Dynamic acceleration signals provide humans with discernible tactile cues up to 1000 Hz [3], and these vibrations are known to play a significant role in a wide range of manual tasks, including tool-mediated perception of surface roughness [13] and dexterous object manipulation [12]. Given the recent proliferation of tiny MEMS-based accelerometers and the importance of these signals for human perception and motor control, one practical approach to improving operator awareness in telemanipulation systems is to provide the operator with haptic feedback of the dynamic acceleration signals experienced by the remote robot, typically by recreating the signals via a voice coil actuator.

This feedback approach has been demonstrated via bench-top research devices [14, 20], and has shown promise for both industrial [7] and medical applications [25, 15, 18]. This approach has also been investigated for improving the tactile sensitivity of hand-held (non-robotic) tools [26]. Additionally, researchers

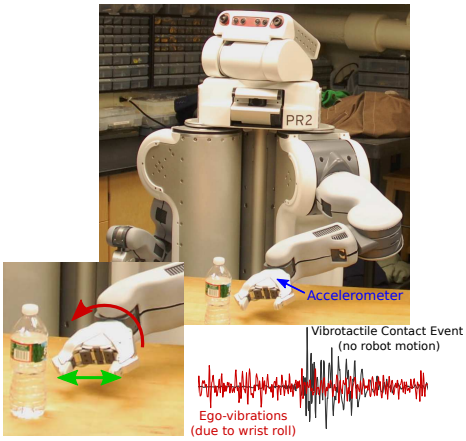


Fig. 1: The Willow Garage PR2 is an example of a modern robotic platform that has high-bandwidth acceleration sensors embedded in its grippers. Gripper joint and wrist roll joint motion are indicated with green and red arrows, respectively. Time series acceleration plots show examples of a clean vibrotactile contact event signal and robot ego-vibrations; the two signals have similar magnitude and spectral content, reducing signal to noise ratio during robot movement.

have developed methods for autonomous robotic manipulation systems to use the perceptual cues provided by vibrotactile acceleration signals (e.g., [9, 22]).

Unfortunately, measurement of tactile acceleration signals can easily be masked or degraded by vibrations that are generated by a robot's own motion, as illustrated in Fig. 1. These "ego-vibrations" often lie within the same frequency range as the external contact signals that one wants to detect for presentation to the human operator or for use in an autonomous robot's controller. Thus the noise-reduction performance of traditional filters (e.g., high-pass, low-pass, notch) is severely limited.

Some previous research in this area has recognized that ego-vibrations mask desired signals and degrade system performance. For example, surgeons using our VerroTouch feedback system occasionally comment that feeling the motion of the da Vinci surgical robot distracts from the vibration cues caused by contact [18]. The primary means of addressing ego-vibrations has been through electromechanical system design. Some researchers have designed custom hardware to mechanically isolate the acceleration sensors from robot motion vibrations [14, 9, 7]. Others have used robotic hardware that is specifically designed for smooth motion, such as Sensable's Phantom Omni haptic device [20, 19]. Others have used their accelerometer only in limited contexts, when they knew that robot motion noise would be small [22].

To improve the performance of vibration feedback systems for teleoperation and to enable measurement of useful high-frequency tactile accelerations on robotic platforms that are not mechanically optimized, we propose a signal processing approach that mirrors human neuropsychology. The human central nervous system is believed to use the motor commands sent to the muscles to predict the sensory consequences of movement. These predictions allow one to distinguish self-produced sensations from those arising from external events [5].

Thus, we propose to use knowledge of robot motion to predict the contribution of ego-vibration noise to the measured acceleration signal, and to remove this contribution through spectral subtraction, a method that was originally

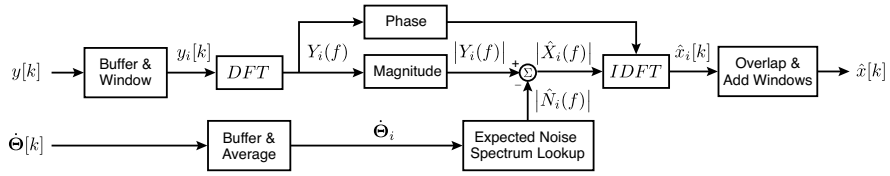


Fig. 2: Block diagram of the spectral subtraction method adapted for ego-vibration suppression in vibrotactile signals.

developed for noise suppression in speech processing [6]. The basic idea of spectral subtraction is that noise in signals can be removed by transforming to the frequency domain and subtracting out an estimate of the noise spectrum. Additionally, Ince et al. have successfully applied this technique to the similar problem of audible robot motion noise in robot audition [10, 11].

The mathematics and signal processing pipeline of spectral subtraction are detailed in Section 2. Section 3 describes our implementation of this approach on a Willow Garage PR2 humanoid robot, which experiences significant ego-vibrations from its wrist roll and gripper joints. We evaluate the performance of this approach in Section 4, and we conclude with Section 5.

## 2 Spectral Subtraction

It is natural to compare vibrotactile acceleration signals to audio signals; the primary way in which these signals differ is in bandwidth. While human skin can perceive vibrotactile cues up to approximately 1000 Hz [3], audio signals are detectable up to 20,000 Hz. Compared to the study of audio signals, the study of vibrotactile acceleration signals is quite immature. Thus we are inspired to look to the audio processing literature, as many of their methods can be directly adapted to handling vibrotactile signals.

The problem of robot ego-vibrations seems most similar to the problem of suppressing additive background noise from a single audio channel of speech. Research into this problem is generally classified as speech enhancement or noise reduction; many of the best methods in this area are reviewed in [23, 4]. Among these approaches, spectral subtraction seems particularly promising for dealing with ego-vibrations because of its straightforward implementation and inexpensive computational requirements that allow for implementation in real-time applications with minimal processing latency.

This section describes our proposed adaptation of spectral subtraction to the problem of ego-vibration suppression in tactile acceleration measurements. Fig. 2 provides a block-diagram illustration of the algorithm. The mathematical notation used here is primarily adapted from [23].

**Block Processing.** Mathematically, noisy observations from an accelerometer can be modeled as

$$y[k] = x[k] + n[k], \tag{1}$$

where $x[k]$ is the vibrotactile event signal, $n[k]$ is additive noise from ego-vibrations, and $k$ is the discrete time index. Following the methods of [16], the multiple orthogonal axes of accelerometer output are combined into a single channel by addition, a computationally simple approach that yields a good spectral match and temporal match with the original signals without introducing any time delay. A band-pass filter then removes both low-frequency cues pertaining to robot motion and high-frequency signals that are not detectable to humans.

The one-dimensional filtered signal is then subjected to block processing [6] as follows:

1. The incoming signal $y[k]$ is buffered into small time buffers $y_i[k]$ of length $L$ that overlap by $M$ samples.
2. Each buffered block $y_i[k]$ is multiplied by a window function $w[k]$ to reduce discontinuities at the end points during discrete Fourier transform (DFT).
3. Each windowed buffer is subjected to spectral subtraction as described in the next subsection.
4. The resultant output signals $\hat{x}_i[k]$ are recombined into the full $\hat{x}[k]$ using the overlap-add method [2].

Typical parameter choices for block processing are 50% buffer overlap ($M = L/2$), and a normalized Hamming window function for $w[k]$. Buffer length choice is a trade-off between frequency resolution and time delay; block processing implementation introduces an algorithm delay of one buffer length.

**Magnitude Subtraction.** After the noisy input signal has been buffered and windowed, each short segment $y_i[k]$ is transformed into the frequency domain using the discrete Fourier transform ($DFT$),

$$y_i[k] \xrightarrow{DFT} Y_i(f) = X_i(f) + N_i(f). \tag{2}$$

The operation of spectral subtraction can be described by the equation

$$|\hat{X}_i(f)| = |Y_i(f)| - |\hat{N}_i(f)|, \tag{3}$$

where $|\hat{X}_i(f)|$ and $|\hat{N}_i(f)|$ are the estimated magnitude spectra of the restored vibrotactile event signal and the noise spectrum respectively. Derivation of the ego-vibration's spectral magnitude estimate $|\hat{N}_i(f)|$ will be discussed in the next subsection. Given the random nature of $N_i(f)$, this operation will sometimes result in negative values for a discrete frequency subband $f$; negative values are consequently set to zero.

Using the phase of the original noisy signal $\Phi_{Y_i}(f)$, which is optimal with regard to minimum mean square error [8], the estimated vibrotactile signal $\hat{X}_i(f)$ can brought back into the time domain as $\hat{x}_i[k]$ via the inverse discrete Fourier transform ($IDFT$),

$$|\hat{X}_i(f)|e^{j\Phi_{Y_i}(f)} \xrightarrow{IDFT} \hat{x}_i[k]. \tag{4}$$

**Noise Spectrum Magnitude Estimate.** While traditional spectral subtraction research has involved developing methods to adaptively estimate the spectrum of an unknown background noise in real-time, when dealing with ego-vibrations we have the luxury of knowing the state of our noise source. A priori observation of the vibrations that occur during unimpeded robot motion can be used to model the expected ego-vibrations during subsequent actions. Depending on the hardware, ego-vibrations might be expected to vary with the robot's joint positions $\mathbf{\Theta}$, joint velocities $\dot{\mathbf{\Theta}}$, and/or joint accelerations $\ddot{\mathbf{\Theta}}$. Thus the ego-vibration magnitude spectrum estimate $|\hat{N}_i(f)|$ in Equation (3) could be a function of all of the robot's present joint states. However, the process of gathering data that fully explores and models the noise spectra that occur in this high-dimensional configuration space would require considerable time and storage capacity. Thus, we seek to reduce the dimensionality of the problem.

Joint acceleration was reported to be unimportant for spectrum estimation of audible joint noise with a Honda ASIMO [10]. Assuming a smooth robotic motion controller, it is reasonable for us to assume that joint acceleration also has little effect on ego-vibrations. For this initial investigation, we have also chosen to neglect the possible influence of joint position. Given our short-time-window implementation, we mark each recorded acceleration sample $y_i[k]$ using the element-wise means of the buffered joint velocity vector $\dot{\mathbf{\Theta}}_i$.

Because we decided to focus on the effects of joint velocity, we designed our estimate of the ego-vibration magnitude spectrum to be

$$|\hat{N}_i(f)| = |\hat{N}(f, \dot{\mathbf{\Theta}}_i)| = \mu_N(f, \dot{\mathbf{\Theta}}_i) + \sigma_N(f, \dot{\mathbf{\Theta}}_i). \tag{5}$$

Here, $\mu_N(f, \dot{\mathbf{\Theta}}_i)$ and $\sigma_N(f, \dot{\mathbf{\Theta}}_i)$ are the mean and standard deviation of the magnitude spectra recorded during a long test at joint velocity vector $\dot{\mathbf{\Theta}}_i$. Other approaches to spectral subtraction sometimes use only the mean value $\mu_N(f, \dot{\mathbf{\Theta}}_\mathbf{i})$. However, empirical results show that some amount of over-subtraction tends to yield better noise suppression in low signal-to-noise ratio (SNR) speech signals [23]. Adding in the standard deviation $\sigma_N(f, \dot{\mathbf{\Theta}}_i)$ allows the degree of over-subtraction to be determined by the variance in a particular frequency sub-band [23].

## 3 PR2 Implementation Details

We tested our full approach to ego-vibration suppression (Fig. 2) using a Willow Garage PR2 humanoid robot.

**Hardware and Algorithm Parameters.** The PR2 was chosen for use in this project because it includes high-bandwidth accelerometers in its sensor suite [1]; as marked in Fig. 1, a three-axis 10-bit digital accelerometer (Bosch BMA150) is embedded within each gripper assembly. Unlike some custom research devices, this robot does not have a wrist-mounted force/torque sensor or all-over pressure-sensitive skin. Instead, the accelerometers are the system's best sensors for dynamic tactile measurements, as demonstrated in [22].

For these initial algorithm-evaluation experiments, we focused on signals from the accelerometer in the right hand. It is subjected to significant ego-vibrations from the nearby wrist rotational joint (roll clockwise/counter-clockwise) and gripper translational joint (close/open). Because the wrist and gripper joints are heavily geared and located so close to the PR2's accelerometer, we believe they are the most challenging and beneficial joints to deal with for ego-vibration suppression. Thus, we define our joint velocity vector as $\dot{\mathbf{\Theta}} = [\dot{\theta}\ \dot{d}]$, where $\dot{\theta}$ and $\dot{d}$ are the wrist roll rotation and gripper translation velocities, respectively.

Experimental data was recorded from the three channels of the accelerometer at a sampling rate of 3000 Hz and a measurement range of $\pm 80$ m/s$^2$ per axis, the maximum specifications of the accelerometer. The corresponding joint velocities, $\dot{\theta}$ and $\dot{d}$, are derived from optical encoder readings and recorded at 1000 Hz.

As described in Section 2, the three acceleration channels were first summed together and band-pass filtered. For the PR2, we employ a fourth-order Butterworth band-pass filter from 150 Hz to 750 Hz; though narrower than the range of human vibrotactile perception, this filtering was chosen to be sure to remove strong signal content observed at 1000 Hz, which likely results from a structural resonance. The just-noticeable difference of human vibrotactile frequency discrimination scales with frequency, resulting in the poorest discrimination at the highest perceivable frequencies; pilot testing of our algorithms with various filter bandwidths indicated that the best perceptual performance occurred when filtering out the 1000 Hz resonance rather than trying to cancel it through spectral subtraction.

Although we evaluated our spectral subtraction algorithm off line, the processed accelerometer readings $y[k]$ and the joint velocity vectors $\dot{\mathbf{\Theta}}[k]$ are fed sequentially into the block process implementation in a manner that is consistent with real-time processing. Block length was chosen to be 64 samples ($L = 64$) with 50% overlap ($M = 32$). At a sampling rate of 3000 Hz, this block length corresponds to an algorithm processing delay of about 21 ms. Studies on human perception of vibrotactile textures [21] and force feedback [24] indicate that delays less than 40 ms are imperceptible, so our processing should not adversely affect the quality of vibrotactile feedback in teleoperated systems.

**PR2 Ego-vibration Estimation.** First, we gathered the data set necessary to compute the velocity-dependent ego-vibration magnitude spectrum estimates $|\hat{N}(f, \dot{\mathbf{\Theta}}_i)|$ defined in Equation (5). Joint velocities were obtained from the ROS Diamondback *pr2_mechanism_model* class, which reports velocities using first-order differentiation of encoder readings. The maximum speed for the wrist roll and gripper joints are 3 rad/s and 0.04 m/s, respectively. All combinations of wrist roll velocity and gripper velocity were sampled at intervals of 10% of the joint's maximum speed, ranging from -100% (wrist rolling clockwise and gripper closing at maximum speed) to 100% (wrist rolling counter-clockwise and gripper opening at maximum speed). Note that these tests included 0% velocities, when the wrist and/or gripper are stationary, to ensure measurement of background accelerometer noise. The data was gathered in semi-continuous 15-second

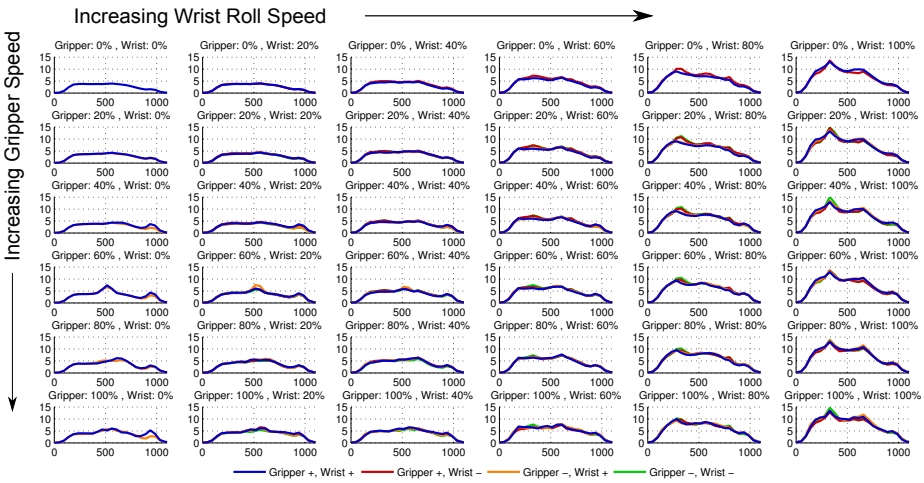


Fig. 3: Plots of the estimated ego-vibration magnitude spectra caused by combinations of gripper and wrist roll speeds. Speeds are defined as a percentage of the joint's maximum speed. The x-axes are frequency (Hz) and the y-axes are amplitude (m/s$^2$). The colored lines show small variations in noise at the four joint velocity direction combinations noted in the legend. Note that the top-left plot shows the background accelerometer noise that is present when the robot is stationary.

chunks; while the PR2's wrist joint is capable of continuous rotation, the gripper velocity command had to be reversed when the gripper reached the limits of its 86 mm translation workspace, so we concatenated multiple acceleration recordings together for most wrist-gripper velocity combinations.

We calculate the magnitude spectrum for the many overlapping short time windows of each recording using the same input buffering and windowing approach described in Section 2, These data points are then used to calculate the mean $\mu_N(f, \dot{\mathbf{\Theta}}_i)$ and standard deviation $\sigma_N(f, \dot{\mathbf{\Theta}}_i)$ of the magnitude spectrum, which are combined to find $|\hat{N}(f, \dot{\mathbf{\Theta}}_i)|$. This procedure provides equal spacing of ego-vibration magnitude spectrum estimates throughout the entire wrist roll and gripper joint velocity space.

Fig. 3 shows the estimated ego-vibration magnitude spectra for a subset of the sampled joint velocities, calculated from equation (5). The mean and the standard deviation of the noise both increase as joint speeds increase. Visual inspection of the recorded time series data and the noise residuals seems to indicate that it is reasonable to assume that vibrations depend only on joint velocities at lower speeds. However as speeds increase, we observed changes in the vibration signal that appear to depend on joint position; we plan to investigate this extension in future work.

**Reducing Dimensionality.** It is important to understand that the size of the velocity configuration space increases exponentially with every new joint that is

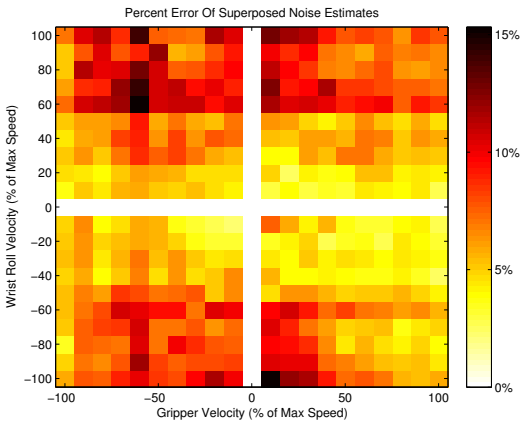


Fig. 4: Percent error between the superposed and observed estimates at different joint velocity combinations.

included in the modeling process. To reduce the testing, calculation, and storage burden of generating spectral magnitude ego-vibration models, we propose that vibration spectra may be superposed (added) across joints. This assumption mirrors the superposition of audio noise assumption made in [11].

Thus for the two-joint case presented in this paper, the noise spectrum is

$$\begin{aligned} |\hat{N}(f, \dot{\mathbf{\Theta}}_i)| &= |\hat{N}(f, [\dot{\theta}\ \dot{d}])| \\ &= \mu_N(f, [\dot{\theta}\ 0]) + \mu_N(f, [0\ \dot{d}]) - \mu_N(f, [0\ 0]) \\ &\quad + \sqrt{\sigma_N(f, [\dot{\theta}\ 0])^2 + \sigma_N(f, [0\ \dot{d}])^2 + \sigma_N(f, [0\ 0])^2}. \end{aligned} \tag{6}$$

This expression represents the noise spectrum at joint velocities $\dot{\theta}$ and $\dot{d}$ as the sum of the noise spectra measured when each joint was moving alone at these velocities, minus the noise spectrum measured when both joints were stationary (since this background noise is presumably present in both of the added signals).

We examined the validity of this assumption by calculating the mean error between the magnitude estimate calculated from equation (6) and the observed magnitude estimate summed over the frequency subbands. Fig. 4 graphically shows the percent error for all 441 joint velocity combinations. The additive models have low error for wrist roll velocities up to about 50% of maximum, but the assumption starts to break down at high wrist roll velocities, reaching errors of 15%. The remainder of this paper employs the superposed noise assumption to test its reasonableness.

## 4 Performance Experiments

This section presents the two experiments we conducted to evaluate the performance of our spectral subtraction noise suppression algorithm during dynamic joint motions. The wrist roll and gripper joints were given random velocity commands that had been low-pass filtered to meet our smooth controller assumption.

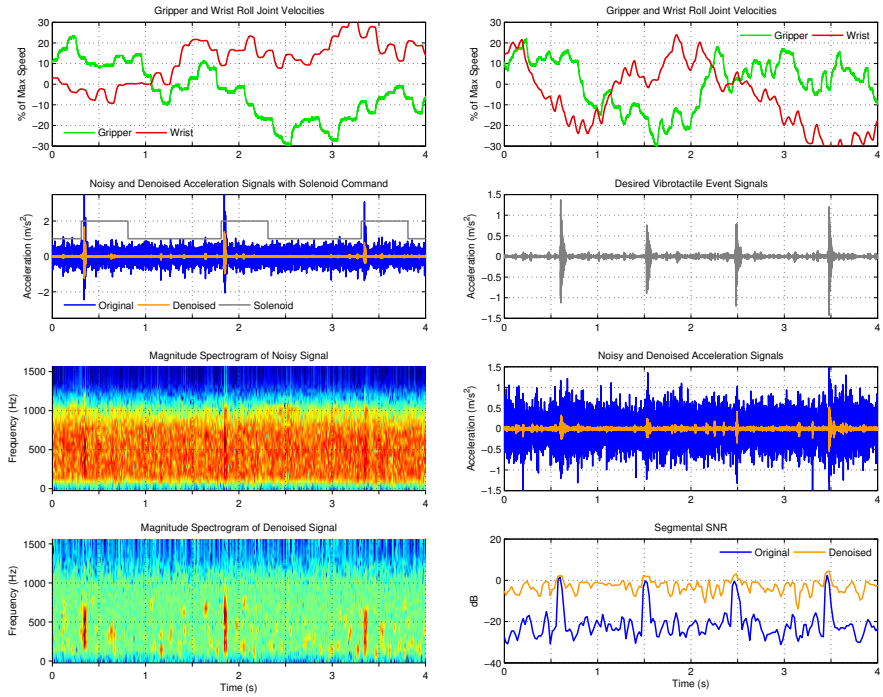


Fig. 5: Results from the solenoid tapper experiment (left) and from adding recorded tap signals to recorded ego-vibration signals (right).

First, a small solenoid (Ledex 174534-035) was used to consistently tap on the PR2's lower arm, near the wrist joint. This setup provides the robot with a consistent vibrotactile event stimulus that simulates the signal it would experience when making contact with its environment.

Results from a trial of this experiment are shown in Fig. 5 (Left). The solenoid taps are visually apparent in the time domain signal and magnitude spectrogram of both the noisy and denoised acceleration signals. However, the denoised signal shows a significant reduction in the noise ceiling of the signals, from a mean signal magnitude of 0.27 $m/s^2$ to 0.02 $m/s^2$. Albeit, this improvement comes at some expense to the magnitude of the tap signal, which features a smaller percentage fall from an average peak magnitude of 3.41 $m/s^2$ to 1.27 $m/s^2$. Using these values, we estimate an improvement in peak signal-to-noise ratio (SNR) from 22 dB to 36 dB.

However, accurately quantifying signal-to-noise ratio improvements requires ground truth knowledge of the desired signal. Unfortunately, the nature of the ego-vibration problem makes it impossible to accurately determine ground truth. For this reason, we generated a data set that replicates the previous experiment using a denoised solenoid event signal that was pre-recorded while the robot was

stationary. We then recorded ego-vibrations from random robot joint motions and added this noise signal to the pre-recorded solenoid tap signals.

The results of processing one of these summed signals are shown in Fig. 5 (Right). In this case, the magnitude of the original taps is similar to the maximum noise magnitude. This test simulates the contact signals that the robot experiences when making very light contact with its environment. Note that using a simple noise threshold here would also destroy the tap signal.

Segmental SNRs were calculated for the noisy and denoised signal for 64 sample segments with 50% overlap. During contact events, the two signals show similar SNRs. However, the denoised signal shows a $\sim$20 dB improvement in SNR when no contact event signal is present. Trials with larger joint velocities showed similar results, but fast joint motion was prone to generating noise spikes that may be falsely perceived by human operators and autonomous magnitude thresholding as tactile event signals.

## 5 Conclusion

This paper developed a spectral subtraction approach to suppressing ego-vibration noise in robotic high-frequency acceleration signals; we used pre-recorded data to estimate the magnitude spectrum of the noise during a range of robot joint velocities and a block processing procedure to remove the estimated noise spectrum from the measured signal. To our knowledge, this is the first work to address the robot motion noise problem in tactile acceleration signals via advanced signal processing rather than mechanical optimization.

This approach was implemented and tested using the gripper translational and wrist roll rotation joints of a Willow Garage PR2. Our results demonstrate that spectral subtraction can significantly improve signal-to-noise ratio (SNR) in high-frequency vibrotactile acceleration signals. This increase in SNR should lead to improved detection of vibrotactile events for both human operators receiving vibrotactile feedback and autonomous robots using a quantitative event-detection criterion, such as signal magnitude or power. Anecdotally, we feel that this algorithm improves the quality of the vibrotactile feedback.

From our experience with telerobotic systems that provide haptic feedback of measured vibrotactile signals [20, 18], we believe that a low noise ceiling can be especially important for usability. We have anecdotally observed that users tend to choose vibrotactile amplification levels that limit the perceptibility of vibration signals during free motion. We attribute this trend to the human sensitivity to haptic noise. As often stated in haptic device design, “free space should feel free” [17]. With a reduced noise floor, users will be more willing to use higher feedback gains, further improving the perceptibility of the signals they feel.

Secondarily, we found that an estimate of the ego-vibration magnitude spectrum that relied only on joint velocities could provide good noise suppression performance, at least at lower joint velocities. A further simplifying step of superposing (adding) noise estimate models across joints also yielded good performance. At larger joint speeds, a higher dimensional model is needed to more

fully capture the behavior of the ego-vibration noise. In future work, we will further seek to improve the noise suppression capabilities of this method through improved modeling of the ego-vibration noise. We will also seek to formally quantify the effects of this approach through task performance experiments by human subjects with and without spectral subtraction of robotic ego-vibrations.

**Acknowledgments.** Research was sponsored by the Army Research Laboratory and was accomplished under Cooperative Agreement Number W911NF-10-2-0016. The authors thank Joseph M. Romano and Benjamin J. Cohen for their assistance with the PR2 and Willow Garage for their loan of a PR2 to the University of Pennsylvania GRASP Laboratory via the PR2 Beta Program.

## References

1. Willow Garage, "Overview of the PR2," Accessed on February 14, 2011, http://www.willowgarage.com/pages/pr2/overview
2. Allen, J.: Short term spectral analysis, synthesis, and modification by discrete fourier transform. IEEE Transactions on Acoustics, Speech and Signal Processing 25(3), 235–238 (June 1977)
3. Bell, J., Bolanowski, S., Holmes, M.H.: The structure and function of Pacinian corpuscles: A review. Progress in Neurobiology 42(1), 79–128 (Jan 1994)
4. Benesty, J., Chen, J., Huand, Y., Cohen, I.: Noise Reduction in Speech Processing, Springer Topics in Signal Processing, vol. 2. Springer-Verlag (2009)
5. Blackemore, S.J., Wolpert, D., Frith, C.: Why can't you tickle yourself? Neuroreport 11, R11–16 (2000)
6. Boll, S.: Suppression of acoustic noise in speech using spectral subtraction. IEEE Transactions on Acoustics, Speech and Signal Processing 27(2), 113–120 (April 1979)
7. Dennerlein, J.T., Millman, P.A., Howe, R.D.: Vibrotactile feedback for industrial telemanipulators. In: Proc. of the Sixth Annual Symposium on Haptic Interfaces for Virtual Environment and Teleoperator Systems, ASME International Mechanical Engineering Congress and Exposition. pp. 107–113 (November 1997)
8. Ephraim, Y., Malah, D.: Speech enhancement using a minimum-mean square error short-time spectral amplitude estimator. IEEE Transactions on Acoustics, Speech and Signal Processing 32(6), 1109–1121 (December 1984)
9. Howe, R.D., Popp, N., Akella, P., Kao, I., Cutkosky, M.R.: Grasping, manipulation, and control with tactile sensing. In: Proc. of the IEEE International Conference on Robotics and Automation. vol. 2, pp. 1258–1263 (1990)
10. Ince, G., Nakadai, K., Rodemann, T., Hasegawa, Y., Tsujino, H., Imura, J.I.: Ego noise suppression of a robot using template subtraction. In: Proc. of the IEEE/RSJ International Conference on Intelligent Robots and Systems. pp. 199–204 (October 2009)
11. Ince, G., Nakadai, K., Rodemann, T., Hasegawa, Y., Tsujino, H., Imura, J.i.: A hybrid framework for ego noise cancellation of a robot. In: Proc. of the IEEE International Conference on Robotics and Automation. pp. 3623–3628 (May 2010)
12. Johansson, R.S., Flanagan, J.R.: Coding and use of tactile signals from the fingertips in object manipulation tasks. Nature Reviews Neuroscience 10, 345–359 (May 2009)

13. Klatzky, R.L., Lederman, S.J.: Perceiving object properties through a rigid link. In: Lin, M., Otaduy, M. (eds.) Haptic Rendering: Algorithms and Applications, chap. 1, pp. 7–19. A. K. Peters (2008)
14. Kontarinis, D.A., Howe, R.D.: Tactile display of vibratory information in teleoperation and virtual environments. Presence: Teleoperators and Virtual Environments 4(4), 387–402 (Aug 1995)
15. Kuchenbecker, K.J., Gewirtz, J., McMahan, W., Standish, D., Martin, P., Bohren, J., Mendoza, P.J., Lee, D.I.: VerroTouch: High-frequency acceleration feedback for telerobotic surgery. In: Kappers, A.M.L., van Erp, J.B.F., Tiest, W.M.B., van der Helm, F.C.T. (eds.) Haptics: Generating and Perceiving Tangible Sensations, Proc. EuroHaptics, Part I. Lecture Notes in Computer Science, vol. 6191, pp. 189–196. Springer (July 2010)
16. Landin, N., Romano, J.M., McMahan, W., Kuchenbecker, K.J.: Dimensional reduction of high-frequency accelerations for haptic rendering. In: Kappers, A.M.L., van Erp, J.B.F., Tiest, W.M.B., van der Helm, F.C.T. (eds.) Haptics: Generating and Perceiving Tangible Sensations, Proc. EuroHaptics, Part II. Lecture Notes in Computer Science, vol. 6192, pp. 79–86. Springer (July 2010)
17. Massie, T.H., Salisbury, J.K.: The PHANToM haptic interface: A device for probing virtual objects. In: Proceedings of the ASME Winter Annual Meeting, Symposium on Haptic Interfaces for Virtual Environment and Teleoperator Systems. Chicago, Illinois (1994)
18. McMahan, W., Gewirtz, J., Standish, D., Martin, P., Kunkel, J.A., Lilavois, M., Wedmid, A., Lee, D.I., Kuchenbecker, K.J.: Tool contact acceleration feedback for telerobotic surgery. IEEE Transactions on Haptics 4(3), 210–220 (May/June 2011)
19. McMahan, W., Kuchenbecker, K.J.: Haptic display of realistic tool contact via dynamically compensated control of a dedicated actuator. In: Proc. of the IEEE/RSJ International Conference on Intelligent Robots and Systems. pp. 3171–3177 (October 2009)
20. McMahan, W., Romano, J.M., Rahuman, A.M.A., Kuchenbecker, K.J.: High frequency acceleration feedback significantly increases the realism of haptically rendered textured surfaces. In: Proc. of the IEEE Haptics Symposium. pp. 141–148 (March 2010)
21. Okamoto, S., Konyo, M., Saga, S., Tadokoro, S.: Detectability and perceptual consequences of delayed feedback in a vibrotactile texture display. IEEE Transactions on Haptics 2(2), 73–84 (April/June 2009)
22. Romano, J.M., Hsiao, K., Niemeyer, G., Chitta, S., Kuchenbecker, K.J.: Human-inspired robotic grasp control with tactile sensing. IEEE Transactions on Robotics PP(99), 1–13 (2011)
23. Vaseghi, S.V.: Advanced Digital Signal Processing and Noise Reduction. John Wiley & Sons Ltd (2000)
24. Vogels, I.M.L.C.: Detection of temporal delays in visual-haptic interfaces. Human Factors: The Journal of the Human Factors and Ergonomics Society 46(1), 118–134 (Spring 2004)
25. Waldron, K.J., Enedah, C., Gladstone, H.: Stiffness and texture perception for teledermatology. Studies In Health Technology And Informatics 111, 579–585 (2005)
26. Yao, H.Y., Hayward, V., Ellis, R.E.: A tactile enhancement instrument for minimally invasive surgery. Computer-Aided Surgery 10(4), 233–239 (2005)